International Journal Of Engineering Research And Development
e- ISSN: 2278-067X, p-ISSN: 2278-800X, www.ijerd.com
Volume 14, Issue 7 (July Ver. I 2018), PP.85-92

Cargo Vehicle Weight Measurement Accuracy And Correction Plan By Weigh-In-Motion Sensor Type

Gyeong-Seok Byun
Korea Institute of Civil Engineering and Building Technology (KICT)
Corresponding Author Gyeong-Seok Byun

ABSTRACT:- Road damage by overload is extremely serious in terms of road maintenance. Roads that should be safe for people's fast traffic can be dangerous, and blocking lanes for restoration may cause inconvenience. To address such problems, many countries are conducting research on the application of weigh-in-motion (WIM) and high-speed weigh-in-motion (HS-WIM), and are actually utilizing these. These facilities require accurate measurement because they are related to crackdowns and play a significant role in preventing road damage. Therefore, the high accuracy of WIM is required, and it is necessary to compare the major sensors that are installed and operated. It is also necessary to correct sensors with relatively low accuracy so that the target evaluation score can be achieved.
Therefore, in this study, mean absolute percent error (MAPE) evaluation was performed for the commonly used sensors, and considerations for correction were derived.
KEYWORDS:- WIM | ITS | Traffic | Cargo | Vehicle Weight

Date of Submission: 09-07-2018 Date of acceptance: 23-07-2018

I. INTRODUCTION

Logistics can be said to be very important economic activities. From a long time ago, roads and nautical charts have been created by logistics, and regions with active exchanges between countries have become silk roads and have enjoyed prosperity. The domestic logistics of South Korea, in particular, are heavily dependent on land transportation. Logistics by cargo vehicles are on a very high level. Therefore, the country builds roads and performs road maintenance work as much as necessary, and is making significant efforts to provide people with sufficient road services. Traffic data are very important in terms of efficient road supply and maintenance. The creation and expansion of roads are determined through the traffic volume, but there are a number of elements that hinder such efforts. The country performs crackdowns to reduce such elements, and tries to secure the designed service lives of roads and reduce the unnecessary maintenance work through the imposition of penalties for road misuse. It goes without saying that roads are closely related to people's safety, and that both convenience and risks are present on roads. Among the risks, road damage caused by overload threatens the people's safety and leads to social loss owing to the unnecessary maintenance cost incurred. It is for this reason that this study was conducted. In this study, the commonly used weigh-in-motion (WIM) sensors the most important sensors installed in WIM to detect the weight of a cargo vehicle were installed, compared, and discussed. In addition, sensors with relatively low accuracy were evaluated by applying correction values.

The purpose of this study was to evaluate sensors under the mean absolute percent error (MAPE) evaluation target of less than 7% in accordance with the COST-323 evaluation criteria, and to achieve the error value of less than 7% for somewhat inaccurate sensors through corrections.

II. REVIEW OF PREVIOUS STUDIES

1. Review of Previous Studies

1.1 Review of previous WIM-related studies

Sun-Min Kwon et al. (20009) developed a high-speed axial load measuring system using two loop sensors, two WIM sensors, and two wandering sensors, and proposed a method of applying this system to overload detection systems. In particular, they proposed a system capable of detecting breakaways by reading the positions of the left and right tires of a cargo vehicle using wandering sensors.

Heung-Bae Gil et al. (2013) analyzed the data of heavy vehicles collected through the use of WIM systems, and classified the commonly used heavy vehicles because the sizes and distribution characteristics of heavy vehicles, such as large cargo vehicles, significantly affect the durability and designed service life evaluation of bridges. The analysis was conducted using the Weibull3 probability distribution model, one of the extremal distribution models.

Ho-Jung Kim et al. (2003) derived vehicle types that exhibit their weight distributions in uniform patterns to improve the efficiency and accuracy of the weight correction of WIM. Through the review of weight distributions, type 6 dump trucks were derived as the most appropriate experimental vehicles.

1.2 Overseas WIM application cases

In Japan, crackdowns are conducted using overload vehicle detection systems linked to video systems. Load detection is performed mainly for vehicles entering the highways from the ports, and the application of high-speed WIM (HS-WIM) systems is being researched on.

In Oklahoma and Kansas in the United States, automatic vehicle identification (AVI) transponders are mounted and operated through electronic toll and traffic management (ETTM) systems. They are operated in the form of automatic detection systems through wireless communication between roadside equipment (RSE). Furthermore, in Connecticut, the weight of a cargo vehicle is inspected through WIM systems. Low-speed WIM (LS-WIM) and HS-WIN systems are constructed and operated.

In Germany, camera-based image recognition systems are used to detect overload among the cargo vehicles running on the Autobahn. Overload is first detected using HS-WIM, and is then confirmed through camera image recognition.

In the Netherlands, the WIM-WID (WIM+Video) system is operated using both HS-WIM sensors and CCTVs. A demonstration interval was constructed to verify this system, and its effects were verified by testing both the piezo method and the bending plate method at the same time.

III. METHODOLOGY

In this study, MAPE evaluation was performed by installing WIM sensors by sensor type. First, the site situations were analyzed to set the installation interval of the WIM sensors. After installation, correction values were obtained considering the pavement state and road surface temperature. When the MAPE value of a specific axle vehicle does not meet the target value, additional corrections were set to achieve the target value. Table 1 shows the characteristics of each sensor.

Table 1. Characteristics of the commonly used WIM sensors

Category	Quartz	Ceramic	Film
Material	Quartz	Ceramic	PVDF polymer
Manufacturing country (manufacturer)	Switzerland (KISTLER)	France (ECM)	United States (MSI)
Measurement range	0-15 tons	-	-
Accuracy	±2% (most accurate)	7% (medium level)	7% (low)
Temperature change error rate	0.02%	-	0.2%
Minimum speed	5 km/h	20 km/h	5 km/h
Operating temperature	-40-80℃	-30-70℃	-40-70℃
Durability	Over 10 years	Over 5 years	40 million times
Market price	Very high	Medium	Low

Prior to the conduct of this study, the site situations were investigated in three steps for the construction of the optimal WIM system. First, the traffic speed for the installation point was investigated, and the international roughness index (IRI: m/km) of the point was measured for use for corrections later. In addition, the frequency of type 4 dump trucks, which are commonly used cargo vehicles, was measured so that the installation of the WIM sensors could be further complemented.

The WIM sensors were installed using the derived WIM sensor interval, and the sensors were evaluated using the mainly used MAPE method. The target value was set to B+ (within 7%), which is the grade that can be used for legal purposes, even though its use requires permission in accordance with COST-323. The equation for MAPE evaluation is equation (1).

$$MAPE = \frac{1}{n}\left(\sum_{i=1}^{n}\left|\frac{X_i - Y_i}{Y_i}\right|\right)\times 100, \quad (1)$$

where X_i = weight value detected from the WIM sensor; Y_i = reference weight value (static weight) of the test vehicle measured with a mobile WIM system (legal meter); and n = number of measurements.

Table 2 shows the evaluation criteria of COST-323, which are the criteria for the target value.

Table 2. Required accuracy and application areas by COST-323 grade

Required accuracy	Application areas and references
A (within 5%)	Legal purposes such as vehicle loading limit and crackdowns
B+ (within 7%)	Legal purposes under specific purposes or permissions
B (within 10%)	Construction of weight information for axles, axle groups, and total weight
C (within 15%) D+ (within 20%)	Statistical data construction, frequency distribution, social overhead capital, defect evaluation, etc.
D (within 25%)	Statistical purposes, economic and technical research, and vehicle type classification
E (over 30%)	Traffic flow composition, load distribution, and frequency research

Axle load detection for MAPE evaluation detects the axle of a vehicle and measures the axle weight at the same time. When a vehicle passes through the sensor section, a signal waveform is generated. The weight is measured using the signal waveform generation graph. Fig 1 shows a representative waveform that is generated when a vehicle passes through the sensor. From this waveform, the axle load can be calculated by integrating the interval from t1 to t2 — the signal waveform with a level higher than the threshold — and obtaining the area.

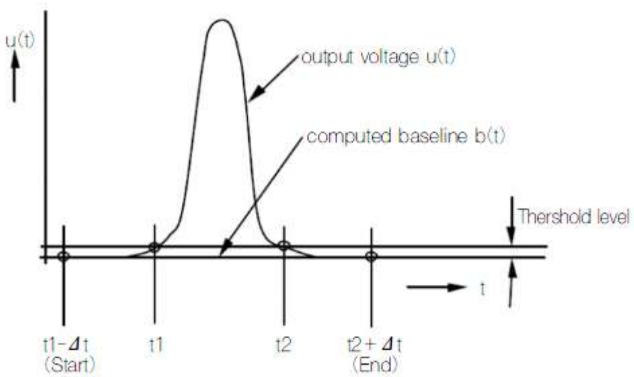

Fig 1. Signal waveform detected by the WIM sensor.

The area from t1 to t2 can be obtained using equation (2).

$$Area = \Sigma \lceil u_i - b_i \rceil , \quad (2)$$

where i = sample number.

After obtaining the area from t1 to t2, the final axle load can be calculated using equation (3).

$$W = \left(\frac{V}{L_s} \right) \times A \times C , \quad (3)$$

where W = axle load; V = vehicle speed; L_s = sensor width; and C = calibration factor.

Finally, the correction factors of the road pavement and the meteorological factor (mainly road surface temperature) sensor were derived using the sequence in Fig 2 to derive the calibration factor (C) for obtaining the MAPE evaluation target of less than 7%. In addition, the WIM sensor was operated 24 hours a day for approximately a month to obtain a more accurate correction factor by securing a large number of specimens. Furthermore, the WIM sensor was corrected using equation (4).

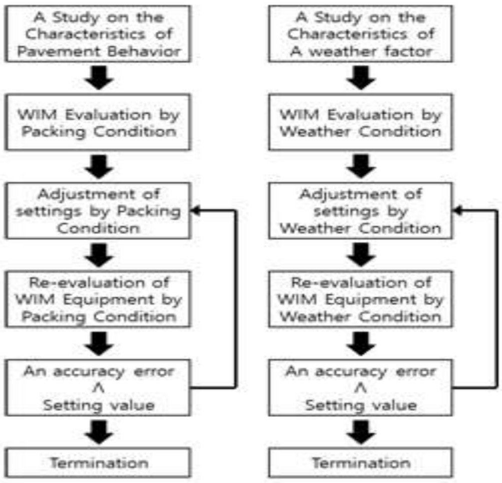

Fig 2. Flowchart for deriving the calibration factor ( ).

In this study, site evaluation was performed to obtain the MAPE evaluation values. Three commonly used cargo vehicle types — the 3-axle cargo truck, 4-axle dump truck, and 5-axle semi-trailer were used. Various axle types were reflected, including the single axle, tandem axle, and tridem axle, to enable diverse evaluation. In addition, measurement was conducted in the morning, in the afternoon, and at night to perform MAPE evaluation and to derive the calibration factor according to the temperature, and measurement was conducted 10-15 times, by applying statistical significance and international criteria. Furthermore, a random number was applied to the weight of each vehicle, and the vehicle weight was varied using the weights before testing for each time zone. The vehicles that were used for testing were weighed three times before evaluation using a vehicle weighing system, and the average values were used as reference values for evaluation.

IV. WEIGHT EVALUATION BY SENSOR

1. Site Situation Survey before WIM Sensor Installation

Prior to the conduct of this study, a three-step process was performed for the optimal WIM sensor installation, and the results shown in Table 3 were derived..

Table 3. Average traffic speed survey results by sensor installation point (km/h)

Category	PVDF(A)	Ceramic	Quartz	PVDF(B)
2-axle vehicle	77	74	63	-
3-axle vehicle	71	72	59	-
4-axle vehicle	70	68	54	56
5-axle vehicle	65	70	49	-
6-axle vehicle	73	72	43	-
Average	71	71	54	56

For the Songgi checkpoint, the average traffic speed was 71 km/h in both directions. For the Seomyeon and Omi checkpoints, the average traffic speed was approximately 55 km/h. Owing to the time limit, the survey was conducted for only an hour, and as such, it is difficult to use the aforementioned values as representative values. Therefore, frequency analysis was conducted based on the 4-axle dump truck the representative heavy cargo vehicle in South Korea to correct the values. Fig 3 show the results of the average speed frequency analysis at each point using the representative vehicle.

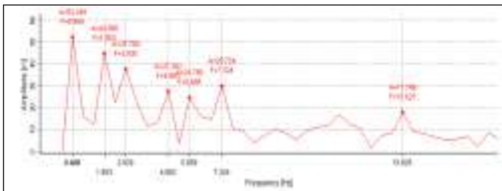

PVDF(A) point single-axle frequency

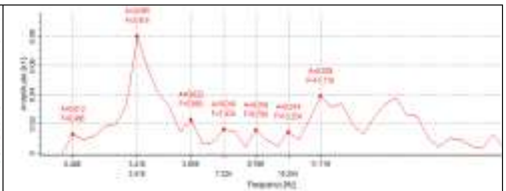

PVDF(A) point tandem axle frequency

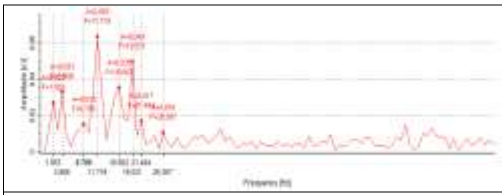

Ceramic point single-axle frequency

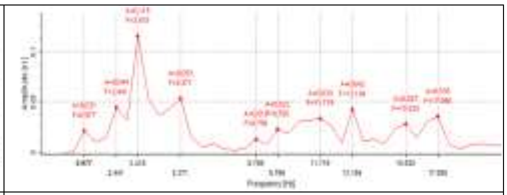

Ceramic point tandem axle frequency

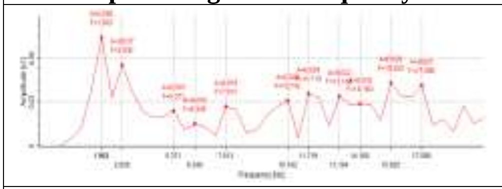

Quartz point single-axle frequency

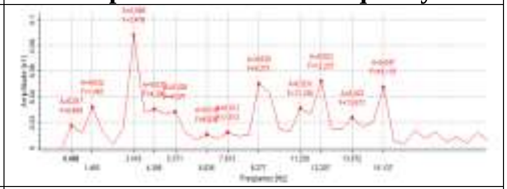

Quartz point tandem axle frequency

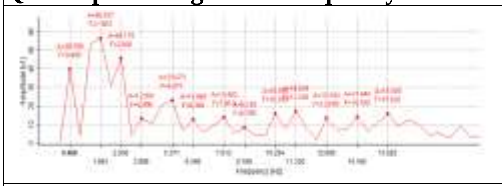

PVDF(B) single-axle frequency

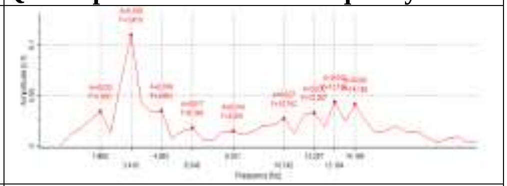

PVDF(B) tandem axle frequency

Fig 3. Single-axle AND Tandem axle frequency by target point.

As can be seen from the analyzed frequencies, the single-axle frequency of the target vehicle was 1.953 Hz, and its tandem axle frequency was 3.418 Hz. The measured IRI value of a newly installed road is considered excellent if it is 2.0 or less. The IRI values of the points other than the ceramic sensor installation point were close to 2.0, and that of the ceramic sensor point was 2.28, which was deemed acceptable for measurement. Therefore, evaluation was performed.

Table 4. IRI value measurement results by point

Category	PVDF(A)	Ceramic	Quartz	PVDF(B)
IRI	1.87	2.28	1.70	2.01

The sensor installation interval was determined using the derived frequency values, average traffic speeds, and IRI values of the road surface at each point, and WIM sensors were installed as follows

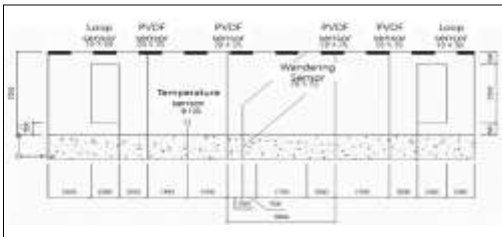

PVDF(A) sensor installation configuration.

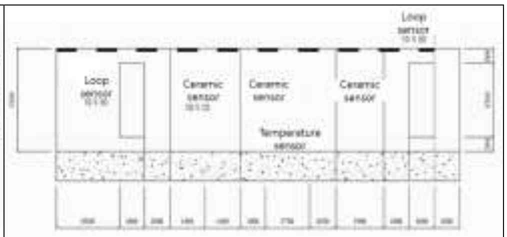

Ceramic sensor installation configuration.

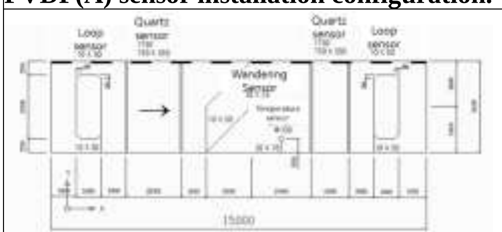

Quartz sensor installation configuration.

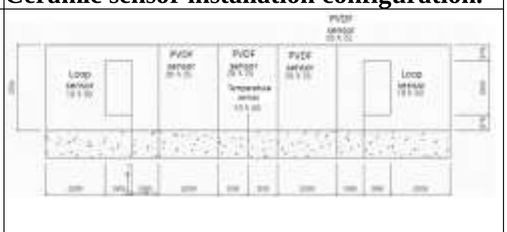

PVDF(B) sensor installation configuration.

Fig 4. Sensors installation configuration.

Table 5. Installed sensors and configurations at each point

Installed sensor	Sensor configuration		Sensor placement
	WIM sensor	Loop sensor	
PVDF	4EA	2EA	Multi-sensors
Ceramic	4EA	2EA	Multi-sensors
Quartz	4EA	2EA	Multi-sensors
PVDF	4EA	2EA	Multi-sensors

As shown in Table 5, multi-sensors were placed at each point, and the sensor configurations were identical. Road surface temperature sensors were additionally installed for road surface corrections according to the temperature.

2. Site Evaluation Results

2.1 MAPE value analysis results by sensor

After the sensors at each point were measured two times and correction values for the sensors and site situations were set through corrections, the results for the final measurement were derived. Below are the first MAPE average values by sensor.

Table 6. Installed-sensor MAPE evaluation for each point

Sensor	Test vehicle	3-axle cargo truck	4-axle dump truck	5-axle semi-trailer
PVDF(A)	1-axle load	11.53	18.92	8.76
	2-axle load	7.22	5.61	22.40
	3-axle load	10.03	6.38	4.95
	4-axle load	-	6.45	45.11
	5-axle load	-	-	49.62
	Total weight	4.23	6.27	20.96
Ceramic	1-axle load	2.71	2.79	14.43
	2-axle load	4.79	5.86	10.92
	3-axle load	10.50	2.73	12.58
	4-axle load	-	3.12	10.96
	5-axle load	-	-	42.25
	Total weight	2.82	2.01	13.09
Quartz	1-axle load	2.91	1.63	4.26
	2-axle load	2.49	3.39	5.13
	3-axle load	5.12	2.02	3.39
	4-axle load	-	2.02	3.36
	5-axle load	-	-	3.45
	Total weight	3.29	1.92	1.57
PVDF(B)	1-axle load	7.70	2.99	3.07
	2-axle load	2.60	4.26	13.08
	3-axle load	2.99	2.23	10.41
	4-axle load	-	5.26	18.29
	5-axle load	-	-	16.55
	Total weight	3.69	1.82	8.01

The MAPE analysis results of each sensor revealed that the values of the quartz sensor were the most excellent. On the other hand, the PVDF and ceramic sensors exhibited MAPE values exceeding 7%, which is the target of the 5-axle semi-trailer, indicating that it was necessary to achieve the target value through corrections. Therefore, in the second site evaluation, the 5-axle semi-trailer that exhibited high MAPE values was evaluated, and the quartz sensor was excluded from the additional corrections and evaluation because its MAPE values were within 7%.

2.2 5-axle semi-trailer axle load correction site evaluation

As the 5-axle values exceeded the target value among the MAPE evaluation results by sensor, MAPE evaluation was performed through corrections based on individual axle loads instead of corrections based on the total weight used for the first evaluation. As the weight corrections of the sensors were performed based on the axle loads, MAPE evaluation was performed twice, with different correction values. The evaluation was performed in the morning, in the afternoon, and at night because corrections were required according to the road surface temperature.

Table 7. 5-axle (semi-trailer) load measurement MAPE evaluation by sensor after corrections

	Evaluation	Total weight	1-axle	2-axle	3-axle	4-axle	5-axle
PVDF (A)	First	3.24	7.19	4.11	2.93	3.06	1.76
	Second	1.03	3.29	3.59	2.00	1.89	0.79
	Average	2.14	5.24	3.85	2.47	2.48	1.28
Ceramic	First	1.70	4.16	2.21	2.00	2.08	2.80
	Second	1.70	2.79	2.32	1.96	1.99	2.49
	Average	1.70	3.48	2.27	1.98	2.04	2.65
PVDF (B)	First	1.99	3.20	2.15	3.43	2.10	2.59
	Second	0.79	3.00	1.45	1.14	1.28	2.24
	Average	1.39	3.10	1.80	2.29	1.69	2.42

As can be seen in Table 5, as the weight measurements of the 5-axle semi-trailer were somewhat higher than the target value according to the first MAPE evaluation results, the 5-axle semi-trailer MAPE values were evaluated by applying the axle loads and correction values instead of the previous total weight.

For the additional adjustment of the correction values, the second evaluation was performed twice. Except for the 5-axle MAPE values of the ceramic sensor, all the MAPE values of all the sensors met the target value. In addition, although not presented in this study, the weight correction based on the axle load, which was effective when applied to the 5-axle semi-trailer, was applied to the 3-axle cargo truck and the 4-axle dump truck, but effective MAPE values could not be derived.

In this study, the accuracy of sensors, which is required for the weight measurement of 3-, 4-, and 5-axle cargo vehicles, was evaluated three times through MAPE. B+ (within 7%) was set as the target value in accordance with COST-323, and the target value was achieved through corrections.

V. CONCLUSION

This study was conducted in the following sequence to achieve the mean absolute percent error (MAPE) evaluation target of less than 7%. Three elements of each point were measured and analyzed for the installation of weigh-in-motion (WIM) sensors, and the average speeds of vehicles were derived first at the points where WIM sensors were to be installed. In addition, the frequency value of the 4-axle dump truck — the mainly used cargo vehicle — was measured and utilized to make the speed values accurate. Furthermore, the international roughness index (IRI) was measured to determine if the road was suitable for evaluation. Based on the IRI value of 2.0, the ceramic installation point exhibited a high value of 2.28, but evaluation was nonetheless performed because such value was deemed acceptable. The installation positions of the WIM sensors by point were set using the previously derived three elements, to prepare for MAPE evaluation. In addition, through the influence of the parameters on the axle load values, the flowcharts for the pavement state and the meteorological state (road surface temperature) — the elements required for deriving the calibration factor (C) — were presented. Furthermore, onsite evaluation was performed under various weights by applying random numbers to the weights of the 3-axle cargo truck, 4-axle dump truck, and 5-axle semi-trailer. The evaluation results revealed that the quartz sensor exhibited error values less than the target value of 7% in most of the evaluations that were done. The derived MAPE evaluation values of the PVDF and ceramic sensors, however, were somewhat high. In particular, as the MAPE value of the 5-axle semi-trailer was evaluated highly, the axle load values of the 5-axle semi-trailer were corrected by applying the calibration factor (C) based on the axle loads by axle instead of total-weight-based measurement. The second MAPE evaluation was performed twice to derive the accurate calibration factor, and excellent MAPE values were derived. As for the sensors, the quartz sensor was found to be the most appropriate WIM sensor because it exhibited excellent evaluation values, but it is more expensive (more than 10 times as expensive as PVDF) than the other sensors. It was found that the other sensors could achieve evaluation results similar to those of the quartz sensor by deriving the calibration factor (C) and performing corrections. The quartz sensor, however, can be a good choice considering its economic efficiency according to the temperature, service life, reinstallation cost, and the fact that crackdown facilities are sensitive facilities.

Although the target MAPE value of less than 7% was derived in this study, the study had significant limitations. In particular, the value of the calibration factor (C) and the calibration value of the WIM controller could not be expressed in this study owing to conflicts of interest with the companies that perform the actual business. This study is significant, however, because it proposed a flow for deriving the calibration factor (C) and derived highly reliable result values by performing MAPE evaluation at an actual site.

In addition, a high cost was incurred owing to the construction of a system for evaluating WIM sensors as well as the use of cargo vehicles for evaluation. Therefore, it was difficult to consider the meteorological changes through long-term MAPE evaluation, and thus, further research on the meteorological changes is required. Furthermore, it is necessary to additionally derive the calibration factor (C) according to the road surface states, such as by rain.

A high cost was incurred by the installation of WIM sensors and the measurement of actual cargo vehicles, and a large amount of information could not be published in this study owing to various conflicts of interest as the study was conducted in cooperation with actual WIM controller providers and sensor installation companies. Therefore, the calibration factor (C) for each sensor could not be published, but the flow of the calibration factor (C) was presented through several considerations. In addition, it appears that this study derived satisfactory results in that it presented considerations for the installation of WIM sensors to make excellent detection possible. More accurate detection will be possible if various parameters and the values of the calibration factor (C) are added through further research, and if road construction is performed considering the installation of WIM sensors.

ACKNOWLEDGMENT

This Research was supported by Korea Institute of Civil Engineering and Building Technology's (KICT) task Non-buried vehicle detail specification extraction device

REFERENCES

[1]. Soon-Min kwon, "Development and Application of the High Speed Weigh-in-motion for Overweight Enforcement," Journal of the Korean Society of Road Engineers, Vol4, No11, pp.69-78, 2009

[2]. D. Gil, "Characteristics of Heavy Vehicles Using Expressway NetworksBased on Weigh -in-motion Data" Journal of the Korean Society of Civil Engineers, Vol33, No5, 1731-1740, 2013

[3]. M. Kim, "A Study of Representative Vehicle for Calibration of WIM(Weigh-In-Motion)" , Vol, No, PP.134-139, 2003.

[4]. D. Han, "Introduction of WIM system and Reform Measuer of Korea WIM Specification" Journal of the Korean Society of Civil Engineers, Vol56, No1, PP.58-68, 2008

[5]. Min-Cheil Soon, An Application Study of HS-WIM System for the concrete pavement, A master's thesis, Seoul Institute of Industrial Technology, 2009

[6]. A Final Report on the Control System of Overloaded Vehicles, Korea Institute of Civil Engineering and Building Technology (KICT), 1995

[7]. A Study on the Standardization of Technology Standards for the Control of Overloaded Vehicles, Korea Institute of Civil Engineering and Building Technology (KICT), 1997

Gyeong-Seok Byun"Cargo Vehicle Weight Measurement Accuracy And Correction Plan By Weigh-In-Motion Sensor Type." International Journal Of Engineering Research And Development , vol. 14, no. 07, 2018, pp. 85-92